A gray-box parameters identification method of voltage source converter using vector fitting algorithm

Zhou, Weihua; Wang, Yanbo; Chen, Zhe

Published in:
Proceedings of 2019 10th International Conference on Power Electronics and ECCE Asia (ICPE 2019 - ECCE Asia)

Publication date:
2019

Document Version
Accepted author manuscript, peer reviewed version

A Gray-Box Parameters Identification Method of Voltage Source Converter Using Vector Fitting Algorithm

Weihua Zhou*, Yanbo Wang†, and Zhe Chen‡
Department of Energy Technology
Aalborg University
Aalborg, Denmark
*wez@et.aau.dk, †ywa@et.aau.dk, ‡zch@et.aau.dk

***Abstract*—This paper presents a vector fitting (VF) algorithm-based gray-box structure and parameters identification method for voltage source converter(VSC). Terminal impedance frequency responses of VSC is first measured by frequency scanning method. Then, these impedance frequency responses are fitted by a polynomial transfer function using VF algorithm. Finally, the theoretical terminal impedance formulas of possible control structures are compared with the fitted transfer function. The actual control structure can be selected, and the actual internal parameters can be identified. Simulation results are given to validate effectiveness of the proposed method. The proposed gray-box method can identify both the circuit and controller information even if no internal information of the VSC is provided by vendors due to industrial confidence. In addition, the effect of measurement noise on parameters identification accuracy can be mitigated by increasing the order of the fitted transfer function.**

***Index Terms*—Gray-box method, parameters identification, vector fitting algorithm, voltage source converter.**

I. Introduction

Renewable energy sources, such as wind power and solar power, have been increasingly penetrating into traditional power systems [1]. Voltage source converters (VSCs), as important interfaces, are widely used to deliver the generated electrical energy to utility grid [2]–[4]. In fact, internal parameters of VSCs are important for instability source identification [5], [6], adaptive control design [7], [8], and condition monitoring and fault diagnosis [9], [10].

However, detailed control structure and parameters of VSCs are difficult to obtain due to manufacture confidence [11], [12]. Parameters perturbation of filter inductance and capacitance may occur due to manufacturing tolerance, aging, variation of operating points and temperature [7].

Internal parameters of VSCs are difficult to obtain in practical system. Various methods have been proposed to estimate or identify internal parameters of VSC [7], [8], [10], [13]–[16]. Based on evaluation of closed-loop transient responses of current controller, the equivalent loss resistance between the inverter and grid is estimated in [13], and both equivalent inductance and resistance between the inverter and grid are estimated in [14], respectively. In addition, active and reactive power based model reference adaptive control (MRAC) approach is used to estimate the equivalent inductance and resistance between the inverter and grid in [8]. Furthermore, grid equivalent, AC filter, switching and conduction loss resistance are estimated by using extended harmonic domain in [15]. However, these aforementioned parameter estimation methods are complicated. In [7], [10], the parameters of L filter and LCL filter can be identified, where pseudorandom binary sequence (PRBS) is injected into current control loop of VSC, and the impedance information is obtained by performing FFT on perturbed voltage and current. However, only circuit parameters can be identified, and controller parameters fail to obtained by the PRBS-based method. A two-step parameters identification method is proposed in [16], where a three-phase fault is used to identify all voltage loop parameters and proportional coefficient of current loop in step 1, and DC voltage reference jump disturbance is injected to identify integral coefficient of current loop and filter inductance in step 2. However, the parameter estimation method is not effective for inverter with LCL filter. In addition, implementation of the two-step identification method is time consuming. In [6], parameters of dc voltage controller, current controller and phase-locked loop (PLL) are identified by equalizing theoretical and measured terminal impedance frequency responses with assumption that the control structure is known. However, the parameters of filter are assumed to be known.

This paper presents a gray-box parameters identification method to identify circuit and controller parameters of VSC based on measured output impedance, where parameters of LCL filter, proportional coefficient of current controller and sampling time can be identified. Small voltage or current perturbation is first injected into point of common coupling (PCC). Terminal impedance frequency responses of VSC is then obtained by performing FFT on perturbed terminal voltage/current and corresponding current/voltage responses. A

This work was supported by the ForskEL and EUDP Project "Voltage Control and Protection for a Grid towards 100% Power Electronics and Cable Network (COPE)" (Project No.: 880063).

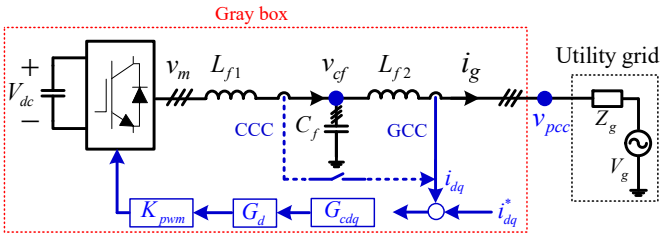

Fig. 1. Gray-box characteristics of the voltage source converter.

polynomial transfer function is then generated by using vector fitting (VF) algorithm on these output impedance frequency responses of VSC. The circuit and controller parameters are then identified from the fitted transfer function based on basic assumption of control structure. The proposed control structure and parameter identification method can be used for oscillation source identification, control optimization design, condition monitoring and fault diagnosis.

The rest of this paper is organized as follows. Section II gives system description. The proposed gray-box parameters identification method is explained in Section III. Section IV provides simulation verification. In addition, impact of measurement noise on identification accuracy is also theoretically analyzed, followed by introducing the corresponding countermeasure. Finally, Section V gives the conclusions.

II. System Description

In this section, the studied power system is first described, followed by introducing two possible terminal impedance formulas of the VSC.

The control diagram of grid-connected inverter is given in Fig. 1. The utility grid is modelled as a Thevenin equivalent circuit consisting of a voltage source V_g in series with an impedance Z_g. The VSC can be enabled by either converter current control (CCC) strategy or grid current control (GCC) strategy. Different control structures have different internal stability regions and terminal impedance characteristics [17], [18].

G_{cdq}, G_d and K_{pwm} are the transfer functions of current controller, digital time delay (T_s is the digital sampling period) and modulator gain, respectively. Their formulas are expressed as follows,

$$\begin{aligned} G_{cdq}(s) &= K_p + \frac{K_i}{s} \\ G_d(s) &= e^{-1.5sT_s} \\ K_{pwm} &= 1 \end{aligned} \tag{1}$$

Then, inverter output impedance under the two control strategies can be derived, shown as (2) and (3) on next page ((3) can be derived as (2) by setting L_{f2} and C_f as zero) [17], [19].

III. The Proposed Gray-Box Parameters Identification Method of VSC

In this section, the VF-based parameter identification method is developed. The principle of the proposed method is first explained, and the detailed implementation procedure of the method is given.

A. Principle of the Proposed Parameters Identification Method

A series of discrete terminal impedance frequency responses can be fitted in s domain using VF algorithm [20], as shown in (4).

$$f(s) = \sum_{i=1}^{m} \frac{R_i}{s - P_i} + D + Es \tag{4}$$

where the fitted transfer function is in m-order partial fraction expansion form. R_i and P_i are the ith residue and pole, respectively. D is the feed-through component, and E is non-zero only if the order of numerator is higher than the order of denominator.

(4) can be transferred into polynomial transfer function form using Matlab command *residue*, shown as (5).

$$f(s) = \frac{\sum_{i=0}^{m} B_i s^i}{\sum_{i=0}^{m} A_i s^i} + Es \tag{5}$$

To extract circuit and controller parameters from the fitted transfer function in (5), the theoretical impedance formulas of VSC under CCC and GCC should also be transferred as polynomial transfer functions. Pade approximation is able to establish an equivalent polynomial function of the digital time delay component G_d [2], shown as (6).

$$e^{-1.5T_s s} = \frac{q_0 + ... + q_i(1.5T_s s)^i + ... + q_l(1.5T_s s)^l}{p_0 + ... + p_j(1.5T_s s)^j + ... + p_k(1.5T_s s)^k} \tag{6}$$

where $p_j = \frac{(l+k-j)!k!}{j!(k-j)!}$, $j = 0, 1..., k$, $q_i = (-1)^i \frac{(l+k-i)!l!}{i!(l-i)!}$, $i = 0, 1..., l$.

In practice, the fitting error of (5) for VSC using order $m = 5$ is small enough [5], [12]. Therefore, appropriate values l and k should be chosen to establish equivalent transfer functions of (2) and (3) with both the orders of numerator and denominator equal to 5.

1) CCC Case: For the CCC case, the order of the numerator is lower than the order of the denominator in the equivalent polynomial transfer function no matter what values l and k are chosen. To establish an equivalent polynomial transfer function of (2) similar with the 5-order transfer function ($m = 5$) of (5), the Pade approximation can be represented with either $l = 5$, $k = 3$ or $l = k = 4$. The two Pade approximations are shown in (7) and (8), respectively.

$$G_{d5,3}(s) \approx \frac{q_5 T_s^5 s^5 + q_4 T_s^4 s^4 + q_3 T_s^3 s^3 + q_2 T_s^2 s^2 + q_1 T_s s + q_0}{p_3 T_s^3 s^3 + p_2 T_s^2 s^2 + p_1 T_s s + p_0} \tag{7}$$

$$CCC: \quad Z_{CCC} = \left.\frac{v_{PCC}}{-i_{GCI}}\right|_{i^*_{dq}=0} = \frac{1}{\frac{1}{K_{pwm}G_{cdq}G_d+L_{f1}s} + C_f s} + L_{f2}s \tag{2}$$

$$GCC: \quad Z_{GCC} = \left.\frac{v_{PCC}}{-i_{GCI}}\right|_{i^*_{dq}=0} = \frac{K_{pwm}G_{cdq}G_d + L_{f1}s}{1 + L_{f1}C_f s^2} + L_{f2}s \tag{3}$$

where $p_3 = 405, p_2 = 4860, p_1 = 22680, p_0 = 40320, q_5 = -45.5625, q_4 = 607.5, q_3 = -4050, q_2 = 16200, q_1 = -37800, q_0 = 40320$.

$$G_{nd4,4}(s) \approx \frac{q'_4 T_s^4 s^4 + q'_3 T_s^3 s^3 + q'_2 T_s^2 s^2 + q'_1 T_s s + q'_0}{p'_4 T_s^4 s^4 + p'_3 T_s^3 s^3 + p'_2 T_s^2 s^2 + p'_1 T_s s + p'_0} \tag{8}$$

where $p'_4 = 121.5, p'_3 = 1620, p'_2 = 9720, p'_1 = 30240, p'_0 = 40320, q'_4 = 121.5, q'_3 = -1620, q'_2 = 9720, q'_1 = -30240, q'_0 = 40320$.

On one hand, the impedance formula of the VSC under CCC can be represented in polynomial function form by combining (7) and (2), shown as (9).

$$Z_{CCC} = \frac{b_5 s^5 + b_4 s^4 + b_3 s^3 + b_2 s^2 + b_1 s + b_0}{a_6 s^6 + a_5 s^5 + a_4 s^4 + a_3 s^3 + a_2 s^2 + a_1 s + a_0} + cs \tag{9}$$

where the coefficients are given in (10) and (11).

$$\begin{aligned} &a_6 = K_p q_5 C_f T_s^5 \quad a_5 = (K_p q_4 T_s^4 + p_3 L_{f1} T_s^3) C_f \\ &a_4 = (K_p q_3 T_s^3 + p_2 L_{f1} T_s^2) C_f \\ &a_3 = p_3 T_s^3 + K_p q_2 C_f T_s^2 + p_1 L_{f1} C_f T_s \\ &a_2 = p_2 T_s^2 + K_p q_1 C_f T_s + p_0 L_{f1} C_f \\ &a_1 = p_1 T_s + K_p q_0 C_f \quad a_0 = p_0 \end{aligned} \tag{10}$$

$$\begin{aligned} &b_5 = K_p q_5 T_s^5 \quad b_4 = K_p q_4 T_s^4 + p_3 L_{f1} T_s^3 \\ &b_3 = K_p q_3 T_s^3 + p_2 L_{f1} T_s^2 \quad b_2 = K_p q_2 T_s^2 + p_1 L_{f1} T_s \\ &b_1 = K_p q_1 T_s + p_0 L_{f1} \quad b_0 = K_p q_0 \quad c = L_{f2} \end{aligned} \tag{11}$$

Then, the circuit and controller parameters can be identified by equalizing (9) with the fitted 5-order polynomial transfer function in (5), shown as (12),

$$\begin{aligned} &L_{f2} = E \quad K_p = \frac{B_0}{A_0} \quad C_f = \frac{A_5}{B_4} \\ &T_s = \frac{16 K_p (\frac{A_1}{B_0} - C_f)}{9} \quad L_{f1} = \frac{B_1}{A_0} + \frac{15 K_p T_s}{16} \end{aligned} \tag{12}$$

On the other hand, the impedance formula of VSC under CCC can also be represented in polynomial function form by substituting (8) into (2), shown as (13).

$$Z_{CCC} = \frac{b'_5 s^5 + b'_4 s^4 + b'_3 s^3 + b'_2 s^2 + b'_1 s + b'_0}{a'_6 s^6 + a'_5 s^5 + a'_4 s^4 + a'_3 s^3 + a'_2 s^2 + a'_1 s + a'_0} + c's \tag{13}$$

where the coefficients are listed in (14) and (15).

$$\begin{aligned} &a'_6 = p'_4 L_{f1} C_f T_s^4 \quad a'_5 = (K_p q'_4 T_s^4 + p'_3 L_{f1} T_s^3) C_f \\ &a'_4 = p'_4 T_s^4 + K_p q'_3 C_f T_s^3 + p'_2 L_{f1} C_f T_s^2 \\ &a'_3 = p'_3 T_s^3 + K_p q'_2 C_f T_s^2 + p'_1 L_{f1} C_f T_s \\ &a'_2 = p'_2 T_s^2 + K_p q'_1 C_f T_s + p'_0 L_{f1} C_f \\ &a'_1 = p'_1 T_s + K_p q'_0 C_f \quad a'_0 = p'_0 \end{aligned} \tag{14}$$

$$\begin{aligned} &b'_5 = p'_4 L_{f1} T_s^4 \quad b'_4 = (K_p q'_4 T_s^4 + p'_3 L_{f1} T_s^3) \\ &b'_3 = K_p q'_3 T_s^3 + p'_2 L_{f1} T_s^2 \quad b'_2 = K_p q'_2 T_s^2 + p'_1 L_{f1} T_s \\ &b'_1 = K_p q'_1 T_s + p'_0 L_{f1} \quad b'_0 = K_p q'_0 \quad c' = L_{f2} \end{aligned} \tag{15}$$

Then, the circuit and controller parameters can be identified by equalizing (13) with the fitted 5-order polynomial transfer function in (5), as shown in (16),

$$\begin{aligned} &L_{f2} = E \quad K_p = \frac{B_0}{A_0} \quad C_f = \frac{A_5}{B_4} \\ &T_s = \frac{4 K_p (\frac{A_1}{B_0} - C_f)}{3} \quad L_{f1} = \frac{B_1}{A_0} + \frac{3 K_p T_s}{4} \end{aligned} \tag{16}$$

It can be seen from (12) and (16) that the derived digital sample time T_s and filter inductor L_{f1} are different even if the polynomial transfer functions (9) and (13) are in the same form. Therefore, it's necessary to choose an appropriate Pade approximation from (7) and (8) to obtain parameters of circuit and controller. It's found that (12) is able to obtain more accurate identification result. Therefore, (7) is used here for the fitted 5-order transfer function ($m = 5$).

2) GCC Case: For the GCC case, if $l = 5, k = 3$, the orders of the numerator and the denominator in the equivalent polynomial transfer function are both equal to 5. The impedance formula of the VSC under GCC can be given in polynomial function form by combining (7) and (3), as shown in (17),

$$Z_{GCC} = \frac{e_5 s^5 + e_4 s^4 + e_3 s^3 + e_2 s^2 + e_1 s + e_0}{d_5 s^5 + d_4 s^4 + d_3 s^3 + d_2 s^2 + d_1 s + d_0} + fs \tag{17}$$

where the coefficients are listed in (18) and (19).

$$\begin{aligned} &d_5 = p_3 L_{f1} C_f T_s^3 \quad d_4 = p_2 L_{f1} C_f T_s^2 \\ &d_3 = p_3 T_s^3 + p_1 L_{f1} C_f T_s \quad d_2 = p_2 T_s^2 + p_0 L_{f1} C_f \\ &d_1 = p_1 T_s \quad d_0 = p_0 \end{aligned} \tag{18}$$

$$\begin{aligned} &e_5 = K_p q_5 T_s^5 \quad e_4 = K_p q_4 T_s^4 + p_3 L_{f1} T_s^3 \\ &e_3 = K_p q_3 T_s^3 + p_2 L_{f1} T_s^2 \quad e_2 = K_p q_2 T_s^2 + p_1 L_{f1} T_s \\ &e_1 = K_p q_1 T_s + p_0 L_{f1} \quad e_0 = K_p q_0 \quad f = L_{f2} \end{aligned} \tag{19}$$

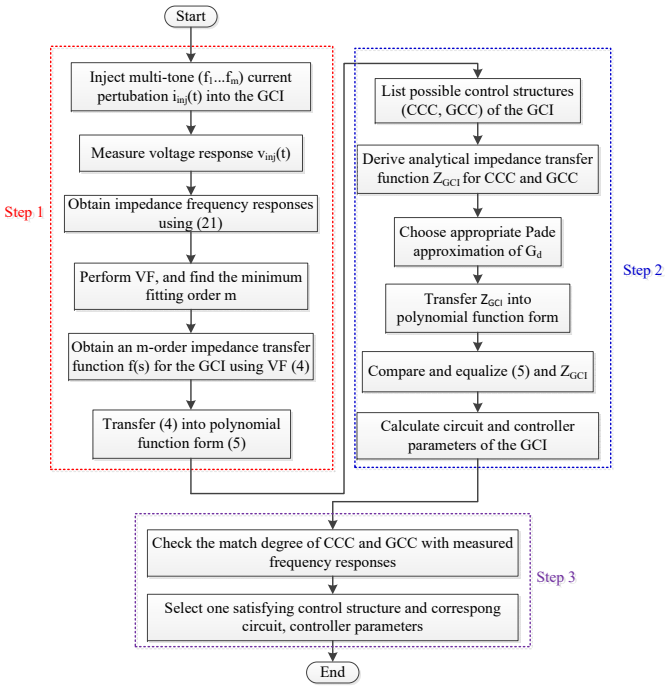

Fig. 2. Flowchart of the proposed control structure and controller parameters identification method of the VSC.

Then, the parameters of circuit and controller can be identified by equalizing (17) with the fitted 5-order polynomial transfer function in (5), as shown in (20),

$$\begin{aligned} L_{f2} &= E \quad K_p = \frac{B_0}{A_0} \quad T_s = \frac{16A_1}{9A_0} \\ L_{f1} &= \frac{B_1}{A_0} + \frac{15K_pT_s}{16} \quad C_f = \frac{A_2}{A_0L_{f1}} - \frac{27T_s^2}{224L_{f1}} \end{aligned} \tag{20}$$

B. Implementation Procedure of the Proposed Method

Fig. 2 shows the proposed control structure and parameter identification method of VSC, which consists of three steps. In step 1, a continuous transfer function of VSC terminal impedance is fitted from a set of measured frequency responses. Fig. 3 shows the terminal impedance frequency response measurement method of VSC. A small current perturbation signal $i_{inj}(t)$ consisting of multiple frequency components $(f_1, f_2...f_m)$ during a frequency range from 400 Hz to 5 kHz is injected into PCC. FFT is performed on the measured terminal voltage $v_{inj}(t)$ and current $i_{inj1}(t)$, and frequency responses of output impedance Z_{VSC} of the VSC can be obtained by dividing $\mathcal{F}(v_{inj}(t))$ by $\mathcal{F}(i_{inj1}(t))$ at these frequency points, as shown in (21) [21].

$$Z_{VSC} = \frac{\mathcal{F}(v_{inj}(t))}{\mathcal{F}(i_{inj1}(t))} \tag{21}$$

Based on the measured impedance frequency response, VF is then used to generate an 5-order transfer function in the form (4). Next, the fitted transfer function in partial fraction expansion form is transferred as polynomial function (5).

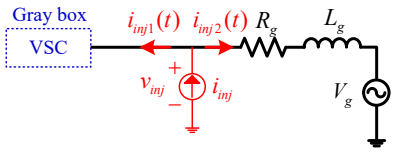

Fig. 3. Terminal impedance frequency response measurement of VSC by injecting small current disturbances.

TABLE I
PARAMETERS OF CIRCUIT AND CONTROLLER FOR FOUR CASES

	VSC parameters			
	#Case 1 (CCC)	#Case 2 (CCC)	#Case 3 (GCC)	#Case 4 (GCC)
V_{dc}	800 V	800 V	800 V	800 V
L_{f1}	3 mH	4 mH	4 mH	2 mH
L_{f2}	2 mH	3 mH	1.6 mH	1 mH
C_f	10 μF	12 μF	5 μF	3 μF
f_{sw}	10 kHz	8 kHz	8 kHz	10 kHz
f_s	10 kHz	8 kHz	8 kHz	10 kHz
K_p	13	15	15	8
K_i	1800	2000	2200	2500
i_d^*	5	5	5	5
i_q^*	0	0	0	0

In step 2, circuit and controller parameters of the VSC is identified from the impedance transfer function fitted in step 1. In detail, possible control structures of the VSC (CCC and GCC) are first listed, and their impedance transfer functions Z_{CCC} and Z_{GCC} are then derived as (2) and (3). The digital time delay G_d is then represented as Pade approximation with appropriate order, and (2) and (3) are transferred into polynomial function form. The two analytical impedance models are compared and equalized with the fitted impedance model (5), and circuit and controller parameters of the VSC can then be identified.

In step 3, match degree of CCC and GCC with the measured frequency responses is checked by comparing non-passivity regions (NPRs) (NPR is the frequency range where phase angle of output impedance is larger than 90^o or lower than -90^o) [18]. Then, the identified system configuration whose NPR fits the measured NPR better is selected.

IV. Simulation Verification

In this section, simulation is implemented to validate the proposed VF-based control structure and parameters identification method. Also, the impact of measurement noise on identification accuracy is investigated.

A. Implementation of the Proposed Method

Simulation verification under different situations is implemented, including different current control strategies (CCC and GCC), different filter parameters, different current controller parameters, and different sampling frequencies. The parameters of circuit and controller are given in Table I.

1) Step 1. Fit Terminal Impedance Frequency Responses Using VF Algorithm: The Bode diagrams of the measured terminal impedance frequency response for #Case 1 within frequency range [400 Hz, 5 kHz] and the fitting results using different orders are given in Fig. 4. It can be seen that fitting

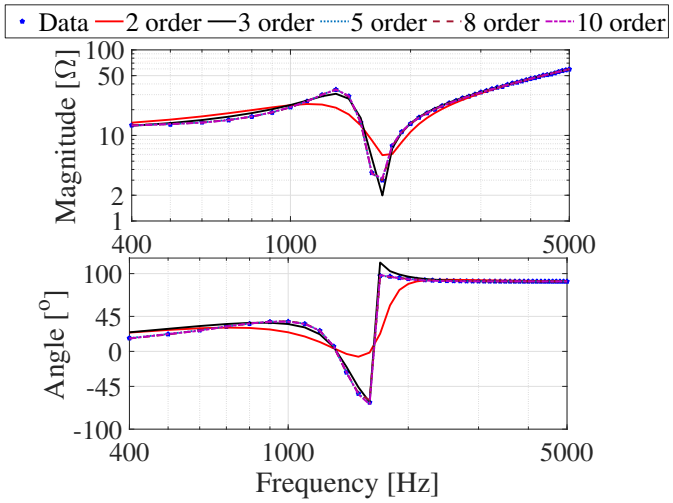

Fig. 4. Fitting results of the measured terminal impedance frequency responses of #Case 1 using different orders.

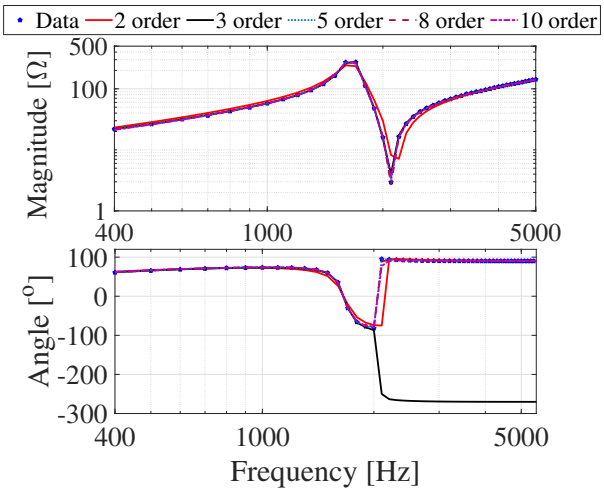

Fig. 5. Fitting results of the measured terminal impedance frequency responses of #Case 2 using different orders.

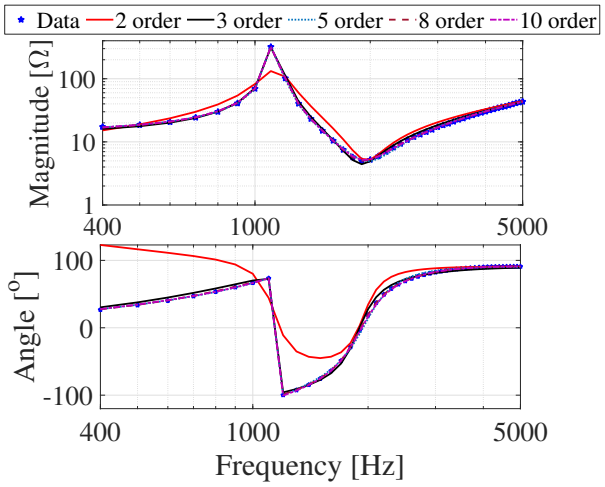

Fig. 6. Fitting results of the measured terminal impedance frequency responses of #Case 3 using different orders.

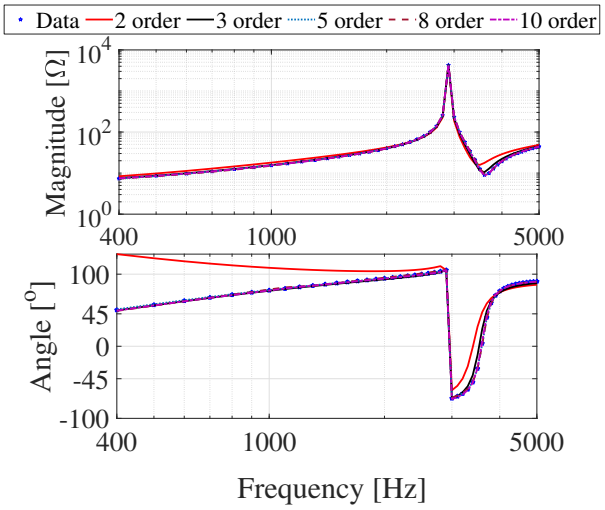

Fig. 7. Fitting results of the measured terminal impedance frequency responses of #Case 4 using different orders.

accuracy can be improved as fitting order increases from 2 to 10. However, the higher order makes the fitted transfer function complicated. In this work, the fitted 5-order transfer function in the form of (5) is used to extract the parameters of circuit and controller. The coefficients of the numerator, denominator and E are given in the first column of Table II.

Similarly, the Bode diagrams of the measured terminal impedance frequency responses for other three cases within frequency range [400 Hz, 5 kHz] and the fitting results using different orders are given in Figs. 5-7. Also, the corresponding coefficients of fitted 5-order polynomial transfer functions are given in the second, third and fourth column of Table II, respectively.

2) Step 2: Identify Control Structure and Parameters of VSC: The VSC can be operated under CCC or GCC mode. The parameters of circuit and controller can be identified by (12) with assumption that the VSC is operated with CCC. Similarly, the parameters of circuit and controller can be identified by (20) with assumption that the VSC is operated with GCC. The control structure and parameters identification procedure of #Case 1 is explained here. For #Case 1, with assumption that the VSC is operated with GCC, the circuit and controller parameters can be calculated by substituting the values in the first column of Table II into (12). The calculated values are given in the first column of Table IV. Then, NPR can be calculated as $f_{NPR} = (1/(6T_s), 1/(2T_s)) = (1727.12, 5181.35)$ Hz. #Case 1 is then assumed to be under GCC mode. The circuit and controller parameters can be calculated by substituting the values in the first column of Table II into (20). The calculated values are given in the second column of Table IV. The NPR can be calculated as $f_{NPR} = (1/(6T_s), 1/(2\pi\sqrt{L_{f1}C_f})) = (509.09, 2080.00)$ Hz.

3) Step 3: Control Structure Selection and Parameters Determination: For #Case 1, $(1727.12, 5181.35)$ Hz agrees with the NPR of the measured data in Fig. 4 (About (1700, 5000)

TABLE II
THE COEFFICIENTS OF THE FITTED 5-ORDER POLYNOMIAL TRANSFER FUNCTIONS (2) FOR FOUR CASES

	The coefficients			
	Case 1 (CCC)	Case 2 (CCC)	Case 3 (GCC)	Case 4 (GCC)
A_5	1	1	1	1
A_4	3.1109e+04	3.1570e+04	1.3283e+05	9.9415e+04
A_3	3.3840e+09	1.9492e+09	4.1688e+09	4.7293e+09
A_2	2.8830e+13	1.2476e+13	6.2110e+13	1.0007e+14
A_1	2.8365e+17	1.0613e+17	2.0588e+17	7.6044e+17
A_0	1.5403e+21	4.1779e+20	2.7729e+21	1.3916e+22
B_5	0.0020	1.9288e-04	-5.0185	-4.9176
B_4	1.0014e+05	8.3395e+04	2.6849e+05	4.6001e+05
B_3	3.0971e+09	2.6239e+09	1.7541e+10	1.8066e+10
B_2	3.3642e+14	1.6121e+14	1.0608e+15	1.9778e+15
B_1	2.7016e+18	9.6008e+17	6.3462e+18	1.6906e+19
B_0	2.0024e+22	6.2668e+21	4.1547e+22	1.1139e+23
E	0.0020	0.0030	0.0016	0.0010

Hz) better than $(509.09, 2080.00)$ Hz. Therefore, the control structure of #Case 1 is selected as CCC, and the parameters can then be determined.

The derivation procedures of the other three cases are similar with #Case 1. The identified parameters are also given in Table IV. It can be seen that the control structures and parameters of different VSCs can be identified.

B. Impact of Measurement Noise on Accuracy of Parameters Identification

To investigate impact of measurement noise on accuracy of parameters identification, 47 random variables $\mathbf{X_{47}}(x_1, x_2, ..., x_{47})$ under normal distribution with mean value 0 and different standard deviations σ from 0 to 1.6 are designed, and added to the 47 analytically derived impedance frequency responses from 400 Hz to 5 kHz Z_{CCC}, shown as follows [22],

$$\begin{aligned} &\mathbf{X_{47}} \sim N(0, \sigma^2) \\ &Z_{CCCp} = Z_{CCC} \times (1 + \mathbf{X_{47}}/100) \end{aligned} \tag{22}$$

where Z_{CCCp} is the measurement value with small disturbance signals, which will be fitted by VF algorithm.

The coefficients of the fitted 5-order polynomial transfer functions in the form of (5) ($m = 5$) are given in Table III. In addition, the circuit and controller parameters are also calculated and listed at the bottom of Table III. It can be seen that the identification accuracy becomes low in the presence of measurement noises. It's because that the fitted low-order transfer function has poor tolerance ability of measurement noise [23].

The coefficients of the fitted 10-order polynomial transfer functions in the form of (5) ($m = 10$) for #Case 1 are given in Table V. To extract circuit and controller parameters from the fitted 10-order transfer function, a new parameters extraction scheme instead of (12) should be adopted. Similar with the parameters identification process for the fitted 5-order transfer function in Section III, l and k in the Pade approximation (6) can be chosen as either $l = m, k = m - 2$ or $l = k = m - 1$ for the m-order transfer function. After repeated test

TABLE III
THE COEFFICIENTS OF THE FITTED 5-ORDER POLYNOMIAL TRANSFER FUNCTIONS IN THE FORM OF (5) ($m = 5$) WITH DIFFERENT MEASUREMENT NOISE AND THE IDENTIFIED PARAMETERS

	Case 1 (CCC) (5 order)				
	$\sigma = 0$	$\sigma = 0.4$	$\sigma = 0.8$	$\sigma = 1.2$	$\sigma = 1.6$
A_5	1	1	1	1	1
A_4	4.1853e+04	-2.9443e+04	-3.0751e+03	-2.4859e+04	-1.3226e+04
A_3	3.1373e+09	1.7661e+09	2.3681e+09	1.6249e+09	2.0446e+09
A_2	2.6904e+13	1.3883e+13	2.0304e+13	1.3817e+13	1.8096e+13
A_1	2.5933e+17	1.5631e+17	2.0386e+17	1.4456e+17	1.7909e+17
A_0	1.3726e+21	9.6834e+20	1.2310e+21	9.6726e+20	1.1833e+21
B_5	3.4681e-04	0.0147	-0.1583	-0.1117	0.2965
B_4	1.0007e+05	9.9386e+04	9.9982e+04	1.0330e+05	1.0997e+05
B_3	4.1753e+09	-3.0019e+09	-8.0411e+08	-2.7571e+09	-1.0421e+09
B_2	3.1137e+14	1.7460e+14	2.4070e+14	1.6642e+14	2.0941e+14
B_1	2.4928e+18	1.3993e+18	1.8709e+18	1.2931e+18	1.6518e+18
B_0	1.7844e+22	1.2601e+22	1.6023e+22	1.2554e+22	1.5217e+22
E	0.0020	0.0020	0.0020	0.0020	0.0020
L_{f2}	2mH	2mH	2mH	2mH	2mH
K_p	13.00	13.01	13.02	12.98	12.86
C_f	$9.99\mu F$	$10.06\mu F$	$10.00\mu F$	$9.68\mu F$	$9.09\mu F$
T_s	$104.92\mu s$	$54.23\mu s$	$63.03\mu s$	$42.34\mu s$	$61.25\mu s$
L_{f1}	3.08mH	2.11mH	2.29mH	1.85mH	2.13mH

and comparison, in the case $m > 10$, identification accuracy is higher if $l = k = m - 1$. p_0, p_1, q_0 and q_1 in (6) can then be calculated as follows,

$$\begin{aligned} p_0 &= q_0 = (2m-2)! \\ p_1 &= (m-1)(2m-3)! \\ q_1 &= -(m-1)(2m-3)! \end{aligned} \tag{23}$$

Then, the circuit and controller parameters can be identified as follows (The detailed derivation process is similar with aforementioned derivation process for $m = 5$, and is omitted here.),

$$\begin{aligned} &L_{f2} = E \quad K_p = \frac{B_0}{A_0} \quad C_f = \frac{A_m}{B_{m-1}} \\ &T_s = \frac{2q_0 K_p(\frac{A_1}{B_0} - C_n)}{3p_1} = \frac{4K_p(\frac{A_1}{B_0} - C_f)}{3} \\ &L_{f1} = \frac{B_1}{A_0} + \frac{3K_p T_s}{4} \end{aligned} \tag{24}$$

The identified circuit and controller parameters using (24) are listed in Table V. It can be seen from Table III and Table V that the fitted 10-order transfer functions can obtain more accurate circuit and controller parameters than the fitted 5-order transfer functions when $\sigma = 0.4, 0.8$ and 1.2. In addition, to obtain a more accurate identification result for $\sigma = 1.6$, higher orders can be used. The identified parameters are given in Table VI when $m = 12, 14, 16, 18$ and 20. It can be seen that these fitted higher-order transfer functions ($m = 12, 14, 16, 18$ and 20) are more accurate than the 10-order transfer function.

Similarly, (20) can also be modified to identify circuit and controller parameters from the fitted higher-order transfer functions for VSC under GCC mode.

TABLE IV
THE IDENTIFIED CIRCUIT AND CONTROLLER PARAMETERS FOR FOUR CASES

	Four VSCs							
	Case 1		Case 2		Case 3		Case 4	
	CCC	GCC	CCC	GCC	CCC	GCC	CCC	GCC
L_{f2}	2mH	2mH	3mH	3mH	1.6mH	1.6mH	1mH	1mH
K_p	13.00	13.00	15.00	15.00	14.98	14.98	8.00	8.00
C_f	$9.99\mu F$	$1.02\mu F$	$11.99\mu F$	$0.61\mu F$	$3.72\mu F$	$4.90\mu F$	$2.17\mu F$	$3.11\mu F$
T_s	$96.50\mu s$	$327.38\mu s$	$131.87\mu s$	$451.61\mu s$	$32.90\mu s$	$131.99\mu s$	$66.21\mu s$	$97.15\mu s$
L_{f1}	2.69mH	5.74mH	4.15mH	8.60mH	2.75mH	4.14mH	1.70mH	1.90mH
f_{NPR1}	1727.12Hz	509.09Hz	1263.87Hz	369.05Hz	5065.86Hz	1117.43Hz	2517.30Hz	1715.38Hz
f_{NPR2}	5181.35Hz	2080.00Hz	3791.61Hz	2190.70Hz	15197.57Hz	1262.72Hz	7551.9Hz	2045.60Hz

TABLE V
THE COEFFICIENTS OF THE FITTED 10-ORDER POLYNOMIAL TRANSFER FUNCTIONS IN THE FORM OF (5) ($m = 10$) WITH DIFFERENT MEASUREMENT NOISE AND THE IDENTIFIED PARAMETERS

	Case 1 (CCC) (10 order)				
	$\sigma = 0$	$\sigma = 0.4$	$\sigma = 0.8$	$\sigma = 1.2$	$\sigma = 1.6$
A_{10}	1	1	1	1	1
A_9	2.7278e+05	4.0656e+04	4.9734e+04	5.9781e+04	3.8977e+04
A_8	5.7949e+10	7.6188e+09	7.8443e+09	7.9267e+09	7.6942e+09
A_7	8.2491e+15	2.8397e+14	3.3077e+14	3.7832e+14	2.6013e+14
A_6	7.5109e+20	1.8244e+19	1.9052e+19	1.9376e+19	1.8013e+19
A_5	5.9001e+25	5.9944e+23	6.8233e+23	7.4068e+23	5.2649e+23
A_4	2.3553e+30	1.5304e+28	1.6107e+28	1.6426e+28	1.3952e+28
A_3	8.9435e+34	3.9382e+32	4.4102e+32	4.5547e+32	3.2603e+32
A_2	7.7218e+38	3.3804e+36	3.7412e+36	3.9325e+36	2.5030e+36
A_1	6.9555e+42	2.8087e+40	3.1684e+40	3.2995e+40	2.3560e+40
A_0	3.4147e+46	1.3439e+44	1.5167e+44	1.6172e+44	7.6583e+43
B_{10}	2.5763e-05	-0.0115	-0.4085	0.4974	-0.4638
B_9	1.0001e+05	9.9339e+04	9.7115e+04	1.0474e+05	1.2420e+05
B_8	2.7276e+10	4.0083e+09	2.3596e+09	8.8876e+09	2.3176e+08
B_7	5.7921e+15	7.5466e+14	7.7857e+14	8.1010e+14	9.3691e+14
B_6	8.2396e+20	2.8207e+19	2.7615e+19	4.2752e+19	1.3652e+19
B_5	7.4916e+25	1.7904e+24	1.8984e+24	1.9427e+24	2.1624e+24
B_4	5.8734e+30	5.9099e+28	6.3555e+28	7.5181e+28	3.7243e+28
B_3	2.3291e+35	1.4613e+33	1.5697e+33	1.6012e+33	1.6438e+33
B_2	8.7607e+39	3.7602e+37	4.1489e+37	4.2911e+37	2.4517e+37
B_1	6.8568e+43	2.8229e+41	3.2095e+41	3.4071e+41	2.7167e+41
B_0	4.4391e+47	1.7374e+45	1.9532e+45	2.0473e+45	9.0312e+44
E	0.0020	0.0020	0.0020	0.0020	0.0020
L_{f2}	2mH	2mH	2mH	2mH	2mH
K_p	13.00	12.93	12.88	12.66	11.79
C_f	$10.00\mu F$	$10.07\mu F$	$10.30\mu F$	$9.55\mu F$	$8.05\mu F$
T_s	$98.26\mu s$	$105.10\mu s$	$101.69\mu s$	$110.84\mu s$	$283.55\mu s$
L_{f1}	2.97mH	3.12mH	3.10mH	3.16mH	6.05mH

TABLE VI
THE IDENTIFIED CIRCUIT AND CONTROLLER PARAMETERS OF #CASE 1 WITH MEASUREMENT NOISE $\sigma = 1.6$ USING DIFFERENT ORDERS

	Case 1 (CCC)				
	$m = 12$	$m = 14$	$m = 16$	$m = 18$	$m = 20$
A_m	1	1	1	1	1
A_1	4.4303e+49	5.4718e+58	4.3222e+67	3.5690e+76	2.5947e+85
A_0	2.1560e+53	2.5508e+62	1.9866e+71	1.6053e+80	1.1162e+89
B_{m-1}	1.0011e+05	9.0716e+04	9.1227e+04	8.9605e+04	8.6642e+04
B_1	4.4514e+50	5.3701e+59	4.2676e+68	3.5466e+77	2.6042e+86
B_0	2.7547e+54	3.3034e+63	2.5656e+72	2.0736e+81	1.4563e+90
E	0.0020	0.0020	0.0020	0.0020	0.0020
L_{f2}	2mH	2mH	2mH	2mH	2mH
K_p	12.78	12.95	12.91	12.92	13.05
C_f	$9.99\mu F$	$11.02\mu F$	$10.96\mu F$	$11.16\mu F$	$11.54\mu F$
T_s	$103.82\mu s$	$95.73\mu s$	$101.33\mu s$	$104.25\mu s$	$109.22\mu s$
L_{f1}	3.06mH	3.04mH	3.13mH	3.23mH	3.40mH

V. CONCLUSION

This paper presents a VF-based parameter identification method which is able to identify control structure, parameters of controller and circuit of VSC. The terminal impedance frequency responses of the VSC is first measured by frequency scanning method. Then, these impedance frequency responses are fitted by a polynomial transfer function using VF algorithm. Finally, the theoretical terminal impedance formulas of possible control structures are compared with the fitted transfer function. The actual control structure can be selected, and the actual internal parameters can be identified. Simulation results show that, with appropriate order choice of Pade approximation for digital time delay, the analytical impedance transfer function can be expressed by a polynomial transfer function, which is in the same form of the fitted polynomial transfer function of the measured terminal frequency responses. Therefore, inverter parameters can be identified by comparing the coefficients of the two polynomial transfer functions. In addition, the effect of measurement noise on identification accuracy can be mitigated by increasing the order of the fitted transfer function. The proposed method is able to identify internal parameters of VSC and contribute to optimized design of controller.

REFERENCES

[1] F. Blaabjerg and K. Ma, "Future on power electronics for wind turbine systems," *IEEE J. Emerg. Sel. Topics Power Electron.*, vol. 1, no. 3, pp. 139–152, Sep. 2013.

[2] Y. Wang, X. Wang, F. Blaabjerg, and Z. Chen, "Harmonic instability assessment using state-space modeling and participation analysis in inverter-fed power systems," *IEEE Trans. Ind. Electron.*, vol. 64, no. 1, pp. 806–816, Jan. 2017.

[3] F. Blaabjerg, Z. Chen, and S. B. Kjaer, "Power electronics as efficient interface in dispersed power generation systems," *IEEE Trans. Power Electron.*, vol. 19, no. 5, pp. 1184–1194, Sep. 2004.

[4] Y. Wang, X. Wang, F. Blaabjerg, and Z. Chen, "Harmonic resonance assessment of multiple paralleled grid-connected inverters system," in *Proc. 2017 IEEE 3rd International Future Energy Electronics Conference and ECCE Asia (IFEEC 2017-ECCE Asia)*, pp. 2070–2075.

[5] M. K. Bakhshizadeh, C. Yoon, J. Hjerrild, C. L. Bak, Ł. H. Kocewiak, F. Blaabjerg, and B. Hesselbæk, "The application of vector fitting to eigenvalue-based harmonic stability analysis," *IEEE J. Emerg. Sel. Topics Power Electron.*, vol. 5, no. 4, pp. 1487–1498, Dec. 2017.

[6] M. Amin and M. Molinas, "A gray-box method for stability and controller parameter estimation in HVDC-connected wind farms based on nonparametric impedance," *IEEE Trans. Ind. Electron.*, vol. 66, no. 3, pp. 1872–1882, Mar. 2019.

[7] D. Martin and E. Santi, "Autotuning of digital deadbeat current controllers for grid-tie inverters using wide bandwidth impedance identification," *IEEE Trans. Ind. Appl.*, vol. 50, no. 1, pp. 441–451, Jan./Feb. 2014.

[8] S. Mukherjee, V. R. Chowdhury, P. Shamsi, and M. Ferdowsi, "Model reference adaptive control based estimation of equivalent resistance and reactance in grid-connected inverters," *IEEE Trans. Energy Convers.*, vol. 32, no. 4, pp. 1407–1417, Dec. 2017.

[9] S. Neshvad, S. Chatzinotas, and J. Sachau, "Wideband identification of power network parameters using pseudo-random binary sequences on power inverters," *IEEE Trans. Smart Grid*, vol. 6, no. 5, pp. 2293–2301, Sep. 2015.

[10] J. Koppinen, J. Kukkola, and M. Hinkkanen, "Plug-in identification method for an LCL filter of a grid converter," *IEEE Trans. Ind. Electron.*, vol. 65, no. 8, pp. 6270–6280, Aug. 2018.

[11] V. Valdivia, A. Lazaro, A. Barrado, P. Zumel, C. Fernandez, and M. Sanz, "Black-box modeling of three-phase voltage source inverters for system-level analysis," *IEEE Trans. Ind. Electron.*, vol. 59, no. 9, pp. 3648–3662, Sep. 2012.

[12] W. Zhou, Y. Wang, and Z. Chen, "Reduced-order modelling method of grid-connected inverter with long transmission cable," in *Proc. 2018 44th Annual Conference of the IEEE Industrial Electronics Society (IECON)*, pp. 4383–4389.

[13] A. Vidal, A. G. Yepes, F. D. Freijedo, J. Malvar, Ó. López, and J. Doval-Gandoy, "A technique to estimate the equivalent loss resistance of grid-tied converters for current control analysis and design," *IEEE Trans. Power Electron.*, vol. 30, no. 3, pp. 1747–1761, Mar. 2015.

[14] A. Vidal, A. G. Yepes, F. D. Freijedo, O. Lopez, J. Malvar, F. Baneira, and J. Doval-Gandoy, "A method for identification of the equivalent inductance and resistance in the plant model of current-controlled grid-tied converters," *IEEE Trans. Power Electron.*, vol. 30, no. 12, pp. 7245–7261, Dec. 2015.

[15] M. Esparza, J. Segundo, C. Gurrola-Corral, N. Visairo-Cruz, E. Barcenas, and E. Barocio, "Parameter estimation of grid connected VSC using the extended harmonic domain," *IEEE Trans. Ind. Electron.*, vol. 66, no. 8, pp. 6044–6054, Aug. 2019.

[16] Z. Liu, H. Wu, W. Jin, B. Xu, Y. Ji, and M. Wu, "Two-step method for identifying photovoltaic grid-connected inverter controller parameters based on the adaptive differential evolution algorithm," *IET Gener. Transm. Distrib.*, vol. 11, no. 17, pp. 4282–4290, Nov. 2017.

[17] W. Zhou, Y. Wang, and Z. Chen, "Frequency and temperature-dependent power cable modelling for stability analysis of grid-connected inverter," in *Proc. 2018 IEEE 4th Southern Power Electronics Conference (SPEC)*, pp. 1–8.

[18] S. G. Parker, B. P. McGrath, and D. G. Holmes, "Regions of active damping control for LCL filters," *IEEE Trans. Ind. Appl.*, vol. 50, no. 1, pp. 424–432, Jan./Feb. 2014.

[19] W. Zhou, Y. Wang, and Z. Chen, "Impedance-based modelling method for length-scalable long transmission cable for stability analysis of grid-connected inverter," in *Proc. 2018 IEEE 4th Southern Power Electronics Conference (SPEC)*, pp. 1–8.

[20] B. Gustavsen and A. Semlyen, "Rational approximation of frequency domain responses by vector fitting," *IEEE Trans. Power Del.*, vol. 14, no. 3, pp. 1052–1061, Jul. 1999.

[21] Y. Wang, X. Wang, F. Blaabjerg, and Z. Chen, "Frequency scanning-based stability analysis method for grid-connected inverter system," in *Proc. 2017 IEEE 3rd International Future Energy Electronics Conference and ECCE Asia (IFEEC 2017-ECCE Asia)*, pp. 1575–1580.

[22] Y. Wang, Z. Chen, X. Wang, Y. Tian, Y. Tan, and C. Yang, "An estimator-based distributed voltage-predictive control strategy for AC islanded microgrids," *IEEE Trans. Power Electron.*, vol. 30, no. 7, pp. 3934–3951, Jul. 2015.

[23] B. Gustavsen, "Improving the pole relocating properties of vector fitting," *IEEE Trans. Power Del.*, vol. 21, no. 3, pp. 1587–1592, Jul. 2006.